



# Pyrolysis of agricultural waste biomass towards production of gas fuel and high-quality char: Experimental and numerical investigations

Agata Mlonka-Mędrala<sup>a,\*</sup>, Panagiotis Evangelopoulos<sup>b</sup>, Małgorzata Sieradzka<sup>a</sup>,  
Monika Zajemska<sup>c</sup>, Aneta Magdziarz<sup>a</sup>

<sup>a</sup> AGH University of Science and Technology, Mickiewicza 30 Av., 30-059 Krakow, Poland

<sup>b</sup> KTH Royal Institute of Technology, Department of Material Science and Engineering, 100 44 Stockholm Brinellvägen 23, Sweden

<sup>c</sup> Czestochowa University of Technology, Faculty of Production Engineering and Materials Technology, Armii Krajowej 19 Av., 42-200 Czestochowa, Poland

## ARTICLE INFO

### Keywords:

Agricultural biomass  
Pyrolysis  
Char  
Tar  
Pyrolytic gas  
Ansys Chemkin-Pro

## ABSTRACT

Biomass wastes are sustainable, renewable, and promising energy sources. In this study, the pyrolysis of agricultural biomass was investigated to determine the most promising process parameters for pyrolytic gas production. The pyrolysis investigations were carried out under nitrogen atmosphere at 300, 400, 500, and 600 °C on the microscale using simultaneous thermal analysis and a laboratory-scale semi-batch vertical reactor. The solid, liquid, and gaseous products were characterised in detail, including the elemental and chemical composition. The gas and liquid products analyses were provided. It was found that the quality of the pyrolytic gas increased with temperature, both in terms of the pyrolytic gas yield and concentration of gaseous components (hydrogen and methane), whereas the carbon dioxide concentration decreased with temperature. The condensed vapours were rich in phenolic and aromatic compounds, and it was noted that the acetic acid concentration increased with temperature. The chemical functional groups in the char were determined using infrared spectroscopy. The carbon content increased with temperature, whereas the hydrogen content decreased. Further decomposition of the organic matrix was observed with increasing temperature. Additionally, chemical modelling of pyrolytic gas was performed using Ansys Chemkin-Pro software and compared with the experimental results. The computational results showed a good correlation with the measured pyrolytic gas composition, especially in the case of the major gas components.

## 1. Introduction

The application of biomass fuels for energy production can contribute to reducing the emission of greenhouse gases and other pollutants, which is essential for reaching recent emission targets [1]. The utilisation of biomass as an energy resource allows us to increase the share of renewable energy sources. The potential of biomass as a renewable energy resource in Poland is high. The estimated surplus biomass potential in the southern and central parts of the country presented in Reference [2] shows that 178,000 t of biomass can be recovered annually for energy purposes, with the assumption that only 30% of surplus biomass is dedicated to this purpose. The most frequently applied thermochemical technologies for converting biomass into energy or chemicals are combustion, pyrolysis, gasification, and high-pressure liquefaction [3]. Due to the low energy density and high moisture and contamination content, waste biomass usually requires

additional treatment, such as thermochemical conversion, to improve its energy properties to meet the requirements for direct combustion [4]. In pyrolysis and gasification technologies, lower-quality fuel is acceptable [5] and pyrolysis is one means of releasing the stored energy within biomass through transformation into other useful products [6]. Pyrolysis is a thermochemical process that relies on the decomposition of biomass in the absence of oxygen [7]. The temperature range for slow pyrolysis of biomass is 300–650 °C, according to the most frequently quoted ranges in the literature presented by Basu [4]. The latest research indicates that the temperature range of this process is considered even broader, from 250 to 900 °C [8]. The pyrolysis process involves very complex and diverse chemical reactions occurring instantaneously [9]. The main part of the process is the thermal cracking reaction in which organic and inorganic gaseous compounds are released during sample heating. The initial products of pyrolysis are condensable gases and solid biochar. Further breakdown of the condensable gas produces the final

\* Corresponding author.

E-mail address: [amlonka@agh.edu.pl](mailto:amlonka@agh.edu.pl) (A. Mlonka-Mędrala).

<https://doi.org/10.1016/j.fuel.2021.120611>

Received 25 October 2020; Received in revised form 25 February 2021; Accepted 3 March 2021

Available online 31 March 2021

0016-2361/© 2021 The Author(s). Published by Elsevier Ltd. This is an open access article under the CC BY license (<http://creativecommons.org/licenses/by/4.0/>).

gaseous products: carbon monoxide (CO), carbon dioxide (CO<sub>2</sub>), hydrogen (H<sub>2</sub>), methane (CH<sub>4</sub>), some higher hydrocarbons such as ethyne (C<sub>2</sub>H<sub>2</sub>), ethylene (C<sub>2</sub>H<sub>4</sub>), ethane (C<sub>2</sub>H<sub>6</sub>), and others, together with liquid products – tars and solid products in the form of char. The yields of the pyrolysis products depend on the biomass composition, especially its hydrogen-to-carbon (H/C) ratio, and process parameters such as the heating rate, pressure, temperature, and residence time. The pyrolysis process is a complex process and depends on many parameters. Validation of the experimental results by means of numerical models enables better understanding of the nature of the process and analysis of the final results with the use of different process parameters. Several studies were dedicated to experimental studies of the waste biomass pyrolysis process, but only few were analysing straw as a feedstock. Kinetic analysis and pyrolysis behaviour were analysed by scientists from India on the example of *Azadirachta indica* and *Phyllanthus emblica* kernel [9]. Wheat, flax, oat and barley straws were considered as a feedstock for catalytic pyrolysis process, but only one process temperature of 500 °C was considered [10]. Similar studies of catalytic pyrolysis at 500 °C, but on example of rice straw, sugar cane bagasse, ugu plant and willow were carried out by Jaffar et al. [11]. The presented studies of straw pyrolysis process revealed that the type of straw has a strong influence on the composition and yield of pyrolysis process products. Numerical assessment of the co-pyrolysis of coal and biomass was studied by Ismail et al. [12], where the modelling results were in good agreement with the experimental results. Numerical studies allow more flexible and detailed combination and analysis of the influence of the process parameters, with parallel analysis of the effect of these parameters on the process. Numerical modelling of the pyrolysis process using Ansys Chemkin-Pro [13] was employed to understand process of product formation, as well as the reaction pathways. Experimental and numerical analyses (using Chemkin-Pro software) of a typical C8 hydrocarbon pyrolysis process were conducted [14], revealing that the fuel structure influences the carbon conversion, along with the process products and yields. For the numerical calculations, the chemical mechanism developed by the Creck Modelling Group was used. The model includes 137 compounds and 4533 chemical reactions and thermodynamic and transport data [15]. The applied model is used for chemical analysis of phenomena and processes occurring during biomass thermal conversion, but it does not take into account the diffusion phenomenon. The mechanism is based on the Arrhenius equations for the reaction constant rate [16]. The proposed mechanism has been used many times in chemical kinetics modelling of the biomass pyrolysis process. Pelucchi et al. presented a kinetic model of pyrolysis biooils [17]. A new characterisation method and a multistep kinetic mechanism for describing the pyrolysis process of algae fuels was proposed by Debiagi and co-workers [18]. Mathematical modelling of fast biomass pyrolysis and bio-oil formation was performed by Ranzi and colleagues [19]. A detailed kinetic model for the combustion of biomass including pyrolysis, gasification, and combustion was presented by Dhahak and co-workers [20]. The correctness of the calculations was validated based on the agreement with the experimental results. In that study, good coherence between the numerical and experimental results was observed. A kinetic model of biomass pyrolysis and secondary cracking was established by Qi et al. [21] to simulate the pyrolysis of biomass, with focus on cracking of the condensable volatile components. That study showed that the numerical results can be validated using thermogravimetric analysis to obtain information for quantitative prediction for small particles (<0.2 mm) and qualitative description for larger particles (<1 mm).

This background demonstrates that there are several studies related to numerical modelling of the pyrolysis process using various models. In those studies, researchers focused mainly on one or two products of the pyrolysis process, especially gaseous or liquid products. The present study is a complex experimental and numerical analysis of the slow pyrolysis process of oat straw. The measurements are focused on the properties and yields of the solid, liquid, and gaseous products, and

advanced analytical methods are included to describe the products of pyrolysis. A kinetic study was performed based on thermal analysis (TA). It was proved in [22], that TA is a powerful technique for kinetics studies of biomass pyrolysis. Fourier-transform infrared spectroscopy (FTIR) analysis was used herein to clarify the chemical structure of oat straw and the produced chars [23]. The tars collected during the experiments were cooled in cold traps and analysed using a gas chromatography - mass spectrometry (GC/MS) liquid analysis system. The chemical composition of the pyrolysis gas was determined using Ansys Chemkin-Pro software and compared with the experimental composition of pyrolysis gas collected from a semi-batch vertical reactor and analysed with a micro-gas chromatograph (micro-GC). The obtained results allowed us to understand the pathway of formation of the gaseous products and to validate the numerical methods by comparison with real experiment. Ansys Chemkin-Pro software enabled the simulation of complex chemical reactions using a variety of chemical reaction mechanisms. In addition, the software enabled fast and accurate kinetic analysis of the reactions and was validated by several scientists for chemical reaction analysis.

Regarding the high potential of biomass in Poland and the increased global interest in the pyrolysis of wastes, the present study, performed for fuel collected from the local market, provides new knowledge regarding a promising technology for biomass waste management on a larger scale. Detailed analysis of the pyrolysis products, together with kinetic modelling, can be used to provide practical descriptors of the conversion process and for optimisation of the reactor design [23].

## 2. Materials and methods

The present study presents a complex analysis of oat straw pyrolysis at four process temperatures: 300, 400, 500, and 600 °C. The details of the experimental and numerical analyses are presented.

### 2.1. Biomass sample

The oat straw is a by-product of production on farmlands and is an agricultural waste with high energy potential. Straw is a very heterogeneous material, and is frequently not appropriate for direct use in combustion power plants because of its low energy density and high content of contaminants [24]. In the present study, agricultural biomass (oat straw) collected from the Polish market was used. The particle size of the studied biomass was < 1 mm.

### 2.2. Proximate and ultimate analyses

Proximate and ultimate analyses of raw biomass were performed according to European Standards (M, moisture content: EN 15934:2012; A, ash content: EN 15403:2011; VM, volatile matter: EN 15402:2011). The same standard was used to determine the volatile matter content of the obtained chars. An elemental analyser was used to determine the carbon, hydrogen, nitrogen, and sulfur content in the raw fuel samples and obtained chars. The oxygen content was calculated. The results of the proximate and ultimate analyses of oat straw are presented in Table 1.

### 2.3. Semi-batch vertical reactor

Lab-scale pyrolysis experiments were conducted in a semi-batch vertical reactor. The pyrolysis of oat straw was carried out under nitrogen atmosphere in the temperature range of 300–600 °C. The temperature range was selected based on the assumption that higher temperatures can enhance the pyrolysis process, but as the energy consumption will also increase, the study was performed up to 600 °C only. Nitrogen was delivered from the top of the reactor and passed through the system at a flow rate of 50 mL/min, controlled by a digital flow meter. Prior to the experiments, the reactor was purged with

**Table 1**

Proximate and ultimate analyses of oat straw in wt.% [25].

| C <sup>daf</sup> | N <sup>daf</sup> | H <sup>daf</sup> | S <sup>daf</sup> | O <sup>daf</sup> | Cl <sup>daf</sup> | M <sup>ar</sup> | A <sup>ar</sup> | VM <sup>ar</sup> | FC <sup>ar</sup> |
|------------------|------------------|------------------|------------------|------------------|-------------------|-----------------|-----------------|------------------|------------------|
| 43.97            | 0.66             | 6.16             | 0.11             | 48.95            | 0.15              | 7.6             | 6.9             | 66.7             | 18.8             |

nitrogen to remove any remaining oxygen. Tars and gases were collected at the bottom of the reactor. During the pyrolysis experiments, vapours were condensed and the released gaseous products were collected in the containers. The collected process gas was split into two separate containers; in the first one, pyrolytic gas released during reactor heat-up was collected, starting from 100 °C up to the selected process temperature. In the second case, the gas produced at the given process temperature was stored. The sample residence time at a given process temperature was 15 min, which was the same in all cases.

#### 2.4. Simultaneous thermal analysis

Thermal analysis (TA) was carried out to investigate the thermal behaviour of oat straw and produced chars. The pyrolysis and combustion processes were investigated. For thermogravimetric analysis (TGA) coupled with differential scanning calorimetry (DSC), the sample was placed in a 70 µL alumina crucible. A fuel sample (5 mg) was heated from ambient temperature to the pyrolysis process temperature at a constant heating rate, the same as that used during the experiments in the reactor, under nitrogen at a flow rate of 50 mL min<sup>-1</sup>. The char produced from the pyrolysis experiments was incinerated afterwards at a constant heating rate of 10 K/min in 50 mL min<sup>-1</sup> under air flow to determine the influence of the pyrolysis process temperature on the properties of the obtained char. The TG and DSC curves for each fuel sample were determined. Based on the TG curves, the mass changes were determined, and DSC was used to determine the thermal effects associated with sample heat-up. Additionally, the first derivative of the TG curves (the DTG) was calculated.

#### 2.5. Infrared spectroscopy analysis

Fourier-transform infrared spectroscopy (FTIR) was used for investigation of the presence of chemical functional groups and identification of the chemical compounds by a Bruker Vertex 70 apparatus. The Bruker Vertex 70 instrument was used for IR analysis of the raw biomass and obtained chars.

#### 2.6. Qualitative analysis of tars

The produced condensable tars were collected in cold traps that were cooled in a bath containing a mixture of water and isopropanol in a 1:1 ratio at 0 ± 1 °C. The weight of the condensed products was first measured using a scale; the samples were then diluted with methanol in a 1:20 ratio and analysed using a GC/MS liquid analysis system (Agilent 7890A gas chromatograph (GC) and Agilent 5975C MSD mass spectrometer (MS)).

#### 2.7. Analysis of pyrolysis gas

The gas collected in the glass containers was analysed using an Agilent 490 Micro-Gas Chromatograph (micro-GC). The micro-GC was equipped with four channels, each of which contained a different column and a thermal conductivity detector. The channels installed were: a Molsieve 5 Å column for detecting the permanent gases: H<sub>2</sub>, He, O<sub>2</sub>, N<sub>2</sub>, CH<sub>4</sub>, CO; a CP PoraPlotU column for separating and determining CO<sub>2</sub>, H<sub>2</sub>S, and C<sub>2</sub> hydrocarbons; a CP PoraPlotU column dedicated to C<sub>3</sub> and C<sub>4</sub> hydrocarbon analysis, and the final column was a CP-Sil 5 CB column for the determination of higher molecular weight hydrocarbons. The carrier gas used in the first two columns was argon, while helium was used in the third and fourth columns. For analysis of the pyrolysis gas,

stable temperature conditions were maintained for two minutes, followed by 30 s of total sampling time.

#### 2.8. Numerical calculations

The present work includes a comparative study of the experimental results with numerical modelling. Understanding and predicting thermal processes are essential for developing competitive technological solutions that aim not only to minimise negative environmental effects, but also to reduce the financial input. Taking into account the technical difficulties related to sample preparation, the performance of instrumental analyses, and the time required for the experiments, numerical modelling seems to be a good alternative for investigating and predicting thermal processes [26].

A perfectly stirred reactor (PSR) was used in the present study, where it is assumed that the process takes place with perfect mixing of the reactants. The same reactor was used by other researchers, and they obtained very good convergence between the calculations and experimental results for pyrolysis [27]. The scheme of the calculation procedure is presented in Fig. 1.

The boundary conditions for the calculations were set based on the experimental parameters. The reaction was performed at temperatures of 400, 500, and 600 °C. The comparative analysis did not include the results at 300 °C because of the limitation of the software; there was no possibility of performing pyrolysis process calculations at temperatures below 370 °C. The process atmosphere was pure nitrogen and the flow rate of nitrogen was set at 50 mL min<sup>-1</sup>; the residence times were the same as in the case of the experiment and varied from 1 to 38 min. The sample mass was also the same as used in the experiment, and was approximately 5 g in all cases.

### 3. Results and discussion

Experimental analysis of the oat straw pyrolysis process in a semi-batch vertical reactor was performed, and complex analysis of all products was performed. Comparative analysis of the experimental and numerical calculation data was also performed.

#### 3.1. Pyrolysis process products yields

The mass balance for the oat straw pyrolysis process (Fig. 2) shows that as the pyrolysis temperature increased, a significant increase in the pyrolytic gas and tar yields was achieved. The yield of gas increased from 13.1% at 300 °C to 16.3% at 600 °C. The solid product yields declined as the temperature increased, and the char concentration increased from 48% at the lowest temperature to 24% at the highest temperature. The mass yields of the liquid products followed a trend similar to that of the pyrolytic gas yield and the highest tar content (57%) was obtained at 600 °C.

#### 3.2. Pyrolysis solid products – char analysis

The results of CHN analysis of the raw oat straw samples and the obtained chars are presented in Table 2. The chars were characterised by a much higher carbon content (68–76%), and the values increased with temperature. During thermal decomposition of the biomass, the hydrogen content of the chars decreased with increasing temperature, where the hydrogen content changed from 4.5% for char obtained at 300 °C to 1.9% for char produced at 600 °C. This change in the biochar composition is consistent with prior experimental results [28]. The

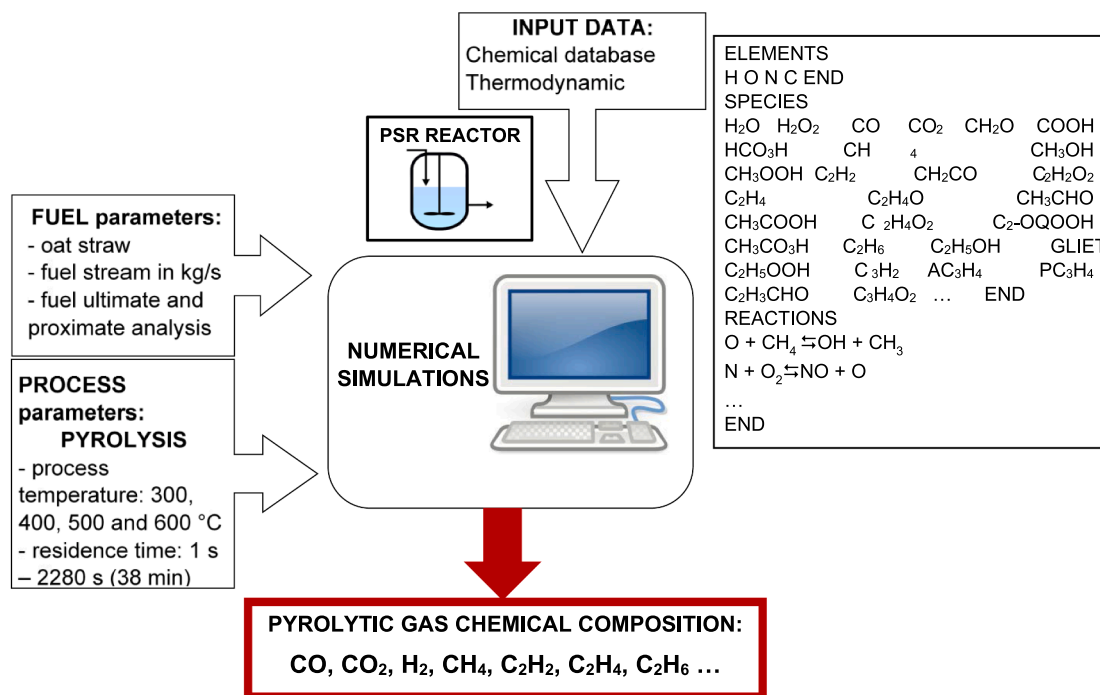


Fig. 1. Scheme of calculation procedure.

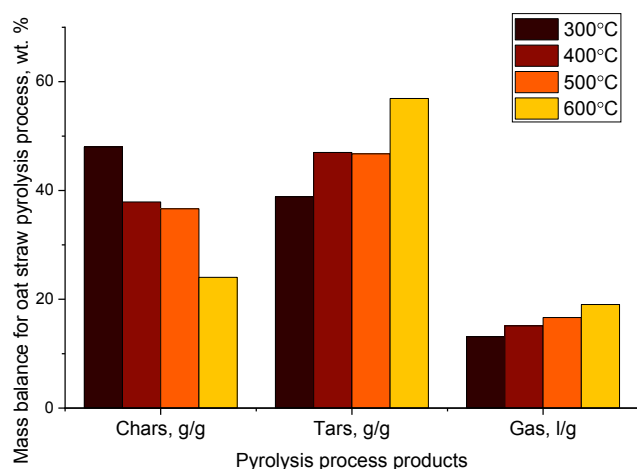


Fig. 2. Mass balance for oat straw pyrolysis process.

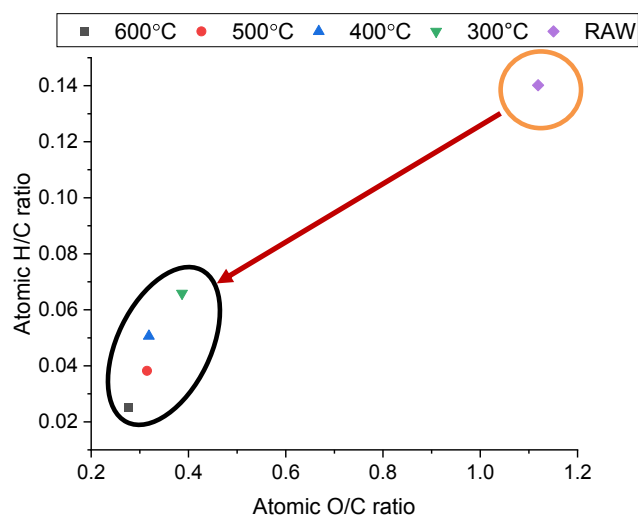


Fig. 3. Van Krevelen chart for raw material and chars obtained under pyrolysis at different temperatures.

Table 2

CHN analysis of raw sample and chars from oat straw, wt. %

| Sample   | C <sup>daf</sup> , % | H <sup>daf</sup> , % | N <sup>daf</sup> , % | O <sup>daf</sup> , % |
|----------|----------------------|----------------------|----------------------|----------------------|
| Raw      | 43.97                | 6.16                 | 0.66                 | 49.21                |
| Char 300 | 67.88                | 4.47                 | 1.38                 | 26.27                |
| Char 400 | 72.17                | 3.65                 | 1.17                 | 23.01                |
| Char 500 | 73.15                | 2.80                 | 1.03                 | 23.02                |
| Char 600 | 76.02                | 1.92                 | 1.07                 | 20.99                |

nitrogen content doubled in comparison to that of the raw fuel sample, but no correlation with the temperature increase was observed.

Fig. 3 shows the relationship between the hydrogen to carbon (H/C) and oxygen to carbon (O/C) molar ratios for the chars and raw fuel samples using the van Krevelen chart. The pyrolysis process strongly reduced the O/C ratio of the raw biomass, and with increasing temperature, the H/C ratio moved towards lower values. Fuels characterised by high H/C and low O/C are generally appropriate for direct fuel

utilisation [29].

Analysis of the volatile matter content in the chars (Fig. 4) shows that at the low temperature of 300 °C, the concentration of volatiles in the chars was still notable and was higher than 35%. The samples prepared at low temperature still contained many volatiles, and the obtained pyrolytic gas did not have good energetic properties. The pyrolysis process at higher temperatures yielded better results.

### 3.3. Simultaneous thermal analysis

Figs. 5 and 6 present the thermogravimetric analysis in the form of TG/DTG and DSC curves for the combustion and pyrolysis studies. Based on these results, it is possible to estimate the differences corresponding to mass changes (TG/DTG) and thermal effects (DSC) during these processes for the studied samples. This method is commonly used to



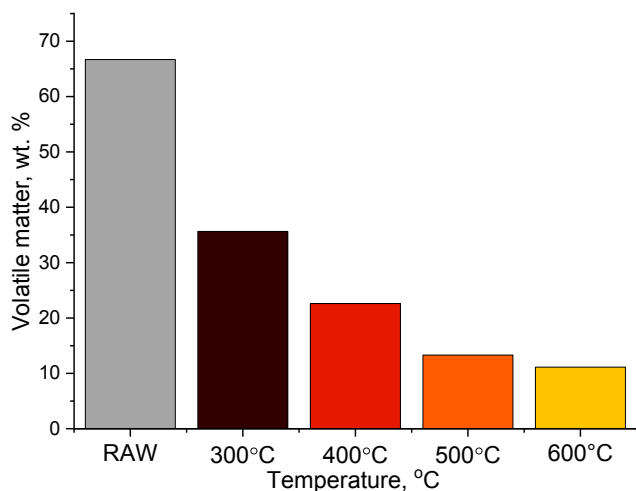


Fig. 4. Combustible and volatile matter content for chars from oat straw, wt.%.

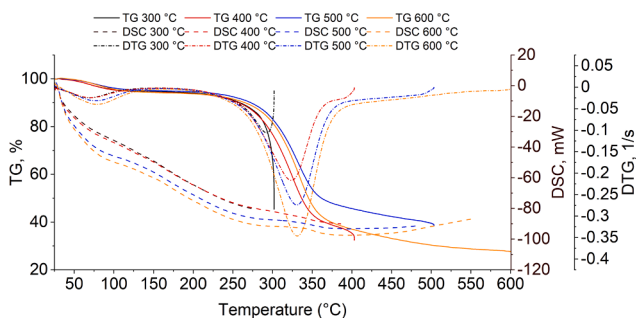


Fig. 5. Thermal behaviour of oat straw under reducing atmosphere/pyrolysis (TG, DTG, and DSC curves).

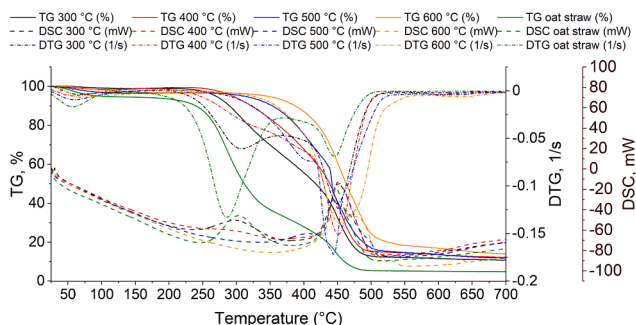


Fig. 6. Thermal behaviour of oat straw raw material and chars under oxidising atmosphere/combustion (TG, DTG, and DSC curves).

study the thermal behaviour of fuels [30].

Analysis of the oat straw pyrolysis process using TGA showed that, as expected, according to the mass balance results, higher temperature favoured raw material decomposition, and the char yield decreased with temperature. The tendencies are similar in all cases (Fig. 5). The pyrolysis process can be divided into two stages. Moisture was first released from the raw material. In the second stage observed within the temperature range of 200 to 450 °C occurred the major mass loss. Only one DTG peak was observed in Fig. 5, which indicates that the decomposition of hemicellulose, cellulose, and lignin overlapped. The thermal decomposition of oat straw up to 450 °C suggests that cellulose and hemicellulose were the main components, and lignin was present in the lowest content. The solid residue generated at 600 °C was 32%.

From analysis of the thermo-chemical decomposition processes of

raw oat straw under an oxidising atmosphere (combustion), it is deduced that the process can be divided into the following stages: drying, devolatilization (low volatile and main volatile), and char oxidation. The first stage takes place up to 120 °C, which is due to water evaporation. The mass loss in this stage was approximately 5%. The volatilization process occurred in the temperature range of 200–350 °C, characterised by a DSC exotherm at 300 °C, typical of lignocellulosic materials, with 60% mass loss. The char oxidation reaction started above 350 °C and a DSC peak was apparent at 451 °C, which may be related to cellulose and lignin decomposition. Above 500 °C, no significant weight loss was observed. The final residue after the thermal decomposition process was 10 wt%. In the case of combustion of the chars from oat straw, above 300 °C, only one peak was observed in the DTG and DSC curves, corresponding to thermal decomposition of the long lignocellulosic chains during the pyrolysis process. For the chars produced at 300 °C, two peaks were observed in the DTG and DSC curves, as thermal decomposition of the sample at this (the lowest analysed) temperature was incomplete. Additionally, with an increase in the pyrolysis process temperature, the ignition point moved towards higher temperatures, which is directly associated with the carbon content in the chars (see Table 2).

### 3.4. Structural analysis

FTIR allowed the identification of the chemical bonds in the raw biomass and chars, and analysis of the changes in functional groups present in the molecules of the studied samples. Based on the FTIR spectra, Table 3 was created to show the impact of the pyrolysis temperature on the molecular structure of the chars. FTIR data were collected in the range of 3500 to 500  $\text{cm}^{-1}$ . The results for raw oat straw were typical for agricultural biomass. For chars, significant changes were observed compared to the features of the initial material. The evident peak at 3340  $\text{cm}^{-1}$  was attributed to the –OH stretching vibration, confirming the presence of water and hydrogen bonds [31]. For the chars, a steady decrease in the intensity of the –OH band was observed with increasing pyrolysis temperature. In the region between 3000 and 2800  $\text{cm}^{-1}$ , two evident peaks at 2925 and 2850  $\text{cm}^{-1}$  were detected for raw biomass. These peaks reflect the asymmetric and symmetric C–H stretching of the methylene groups [32]. It is known that these carbon components are present in cellulose-based materials that are not stable at high temperatures [33]. In the studied temperature range, the intensity of these peaks decreased for the chars prepared at 300 and 400 °C, and disappeared for the chars obtained at 500 and 600 °C. For raw biomass, the stretching vibration of C=O in the ketone and amide groups was detected. The typical C–O stretching bands of cellulose (at 1112  $\text{cm}^{-1}$  and 1032  $\text{cm}^{-1}$ ) appeared and became sharper. This suggests significant removal of hemicellulose, accompanied by increasing cellulose and lignin content in the obtained chars. The absorption band at 898  $\text{cm}^{-1}$  was associated with the C–O–C stretching of the  $\beta$ -glucosidic linkages. This band was observed for raw biomass, and the aliphatic C–H deformation vibrational band (at 1380  $\text{cm}^{-1}$ ) of cellulose and hemicellulose intensified for the chars and decreased with carbonisation [34].

Increasing the pyrolysis temperature caused significant changes in the intensity of the peaks at 3340  $\text{cm}^{-1}$  (–OH) and 1030  $\text{cm}^{-1}$  (C–O) and c.a. 800  $\text{cm}^{-1}$  (C–H). The bonds changed from C–O to O–CH<sub>3</sub>/C–OH and symmetric C–H stretching to lone C–H and O–H stretching.

### 3.5. Pyrolysis vapour products – tar analysis

One of the pyrolysis products is the liquid fraction, called tar or bio-oil. It is a mixture containing condensable hydrocarbons such as complex polyaromatic hydrocarbons and 1- to 5-ring aromatics. Tar can also be defined as all pyrolysis products with molecular weights higher than that of benzene. During the pyrolysis process, tar generally condenses in the colder lower section of the installation [4].

**Table 3**

FTIR data for raw biomass and chars. The location of bands corresponding to the vibration and assignment to functional groups and components were defined based on references [23,31–37].

| Location wavenumber, $\text{cm}^{-1}$ | Functional group (bonds)  | Raw | Char 300 | Char 400 | Char 500 | Char 600 |
|---------------------------------------|---|-----|----------|----------|----------|----------|
| 3340                                  | –OH stretching vibration in hydroxyl or carboxyl groups                                       | +   | +        | –        | –        | –        |
| 3000–2800                             | with aliphatic carbon $-\text{CH}_x$ stretching vibration                                     | +   | +        | +        | –        | –        |
| 2925, 2850                            | asymmetric and symmetric $-\text{C}-\text{H}$ stretching of methylene groups                  | +   | +        | +        | –        | –        |
| 1645                                  | stretching vibration of $-\text{C}=\text{O}$ in ketone and amide groups                       | +   | –        | –        | –        | –        |
| 1590                                  | asymmetric stretching of $-\text{C}=\text{O}$ in carboxylic groups                            | +   | +        | +        | +        | –        |
| 1455                                  | $-\text{C}=\text{C}$ stretching in aromatic ring carbons                                      | +   | –        | –        | –        | –        |
| 1380                                  | aliphatic $\text{C}-\text{H}$ deformation vibrational band                                    | +   | +        | +        | +        | +        |
| 1112                                  | asymmetrical $\text{C}-\text{O}-\text{C}$ stretching  | +   | +        | –        | –        | –        |
| 1030                                  | $-\text{C}-\text{O}-\text{R}$ in aliphatic ethers and alcohol $-\text{C}-\text{O}$ stretching | +   | +        | +        | –        | –        |
| 1021 to 1039 $\text{cm}^{-1}$         | relate to the $\text{C}=\text{C}$ , $\text{C}=\text{O}$ and $\text{C}-\text{OH}$              |     |          |          |          |          |
| 899                                   | $\text{C}-\text{O}-\text{C}$ stretching of $\beta$ -glucosidic                                | +   | +        | +        | +        | +        |

The amount of identified chemical compounds in the tars decreased with increasing temperature. Temperature had an influence on the composition of the liquid pyrolysis products and concentration. With increasing temperature, the tars became more concentrated and less diverse [38]. The following numbers of chemical compounds were detected for each investigated temperature: 300 °C – 38, 400 °C – 33, 500 °C – 30, and 600 °C – 26. The collected tars consisted of a light fraction, which has a light yellowish colour, and a heavy fraction with a dark-brown colour [39].

The detected compounds and their intensities are presented in Fig. 7. For further analysis, compounds with the highest intensity were chosen. At all the chosen temperatures, two main tar components were detected: acetic acid and isobutyric acid. The peak area for acetic acid increased from 11% to 16% with an increase in temperature. The peak area for isobutyric acid decreased from 16.6% at 300 °C to 15.8% at 600 °C. This is due to the nature of this amide, which decomposes around 400 °C [40], subsequent to the formation of acetic acid from the three main compounds of biomass, namely cellulose, hemicelluloses, and lignin. Isobutyric acid was transformed via hydrolysis of the liquid phase pyrolysis products [41]. The obtained phenols were the largest group obtained in the liquid fraction during the experiments. The phenolics group included the following components: phenol, 2-methoxy-phenol, 2,6-dimethoxy-phenol, 2-methoxy-4-vinylphenol, and hydroquinone. The yield of phenol compounds did not change significantly from 300 to 500 °C, as these compounds have high thermal stability and decompose

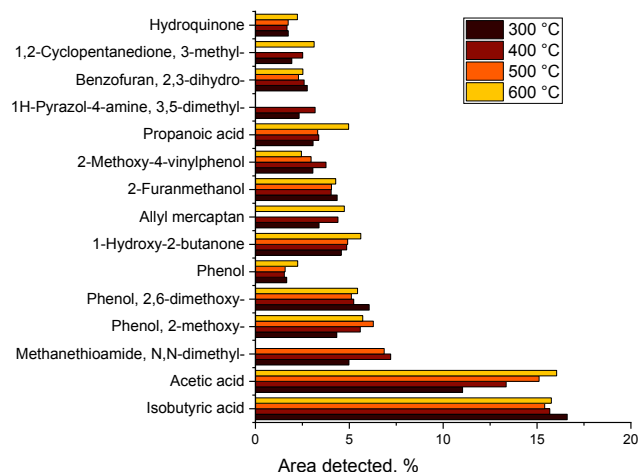


**Fig. 7.** Analysis of tars from pyrolysis experiments at 300, 400, 500, and 600 °C.

above 650 °C [42]. Some of the other phenol group compounds started to decompose above 450 °C, which resulted in a change in the quantity of the whole phenol group [43]. This group was a significant part of the produced tars, as also reported in other studies [44].

### 3.6. Pyrolysis gas products

The pyrolysis gas for both samples collected during each experiment were analysed. The first measurement was performed during reactor heat-up, before reaching the selected temperature of the experiment, and the second was performed at a given process temperature. The Py-gas composition is presented in Figs. 8 and 9.

The pyrolysis gas formed during reactor heat-up consisted mainly of  $\text{CO}_2$  and  $\text{CO}$ , and its concentration increased with temperature. During the temperature increase, the structure of the biomass was modified and the chemical components of the biomass decomposed. Hemicellulose was removed, and cellulose and lignin were dehydrated and partially reduced, resulting in enhanced release of  $\text{CO}$  and  $\text{CO}_2$  [45]. At lower temperatures, hydrogen and ethylene were not detected.

Methane release is associated with cracking of the methoxy group ( $-\text{O}-\text{CH}_3$ ) when the temperature is lower than 600 °C. This process takes place during the primary and secondary pyrolysis stages at temperatures ranging from 200 °C to 600 °C [46]. The most promising

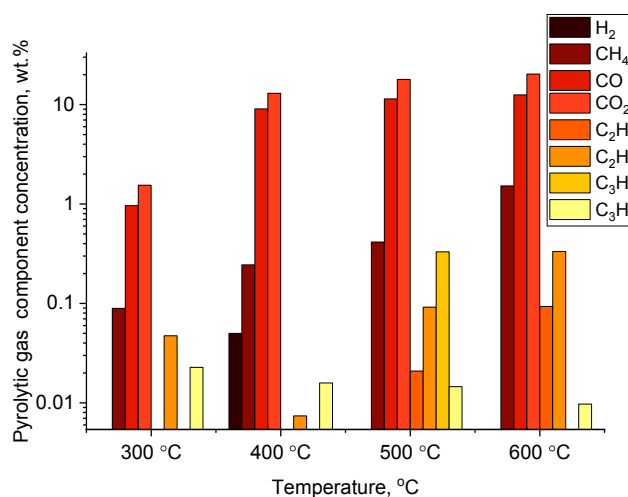


**Fig. 8.** Analysis of gas from oat straw before reaching pyrolysis temperature, in %.

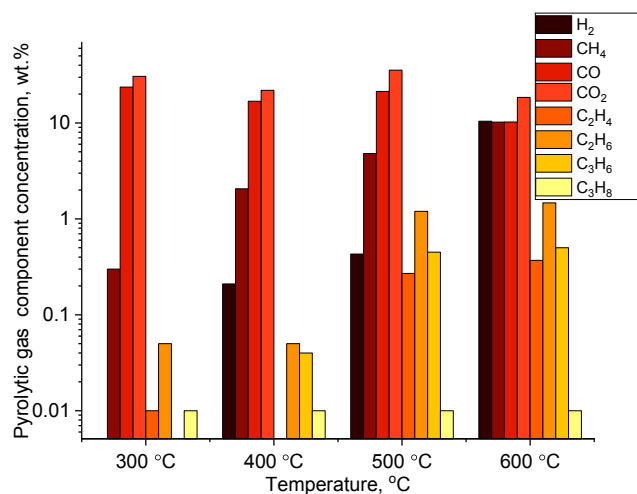


Fig. 9. Analysis of gas from oat straw after reaching pyrolysis temperature.

composition of Py-gas was observed in the case of the highest process temperature, where the highest content of the most valuable gas products, such as hydrogen and methane, was obtained. A rapid increase in the hydrogen yield at 600 °C was observed. The release of H<sub>2</sub> is related to the deformation of aromatic bonds such as C–H and C = C, as well as the decomposition of polymers [46]. The contents of C<sub>2</sub>H<sub>4</sub>, C<sub>2</sub>H<sub>6</sub>, and C<sub>3</sub>H<sub>6</sub> obtained at the highest temperature were 0.37%, 1.47%, and 0.5%, respectively.

### 3.7. Numerical calculation of pyrolysis gas products

The numerical studies allowed calculation of the concentration of gaseous species generated during the pyrolysis process. The main gaseous species are compared to the experimental results (H<sub>2</sub>, CH<sub>4</sub>, CO, CO<sub>2</sub>, C<sub>2</sub>H<sub>4</sub>, C<sub>2</sub>H<sub>6</sub>, C<sub>3</sub>H<sub>6</sub>, and C<sub>3</sub>H<sub>8</sub>) in Fig. 10.

Comparative analysis showed good correlation between the experimental results and calculations. Some inconsistencies in the correlation were observed for H<sub>2</sub> and higher hydrocarbons such as C<sub>2</sub>H<sub>4</sub>, C<sub>2</sub>H<sub>6</sub>, C<sub>3</sub>H<sub>6</sub>, and C<sub>3</sub>H<sub>8</sub>. Because higher hydrocarbons are present in pyrolytic gas in trace amounts, the detection of these species was encumbered by high measurement uncertainty. Additionally, the differences could result from the impact of the presence of other higher hydrocarbons, the concentration of which was calculated in the numerical model: C<sub>6</sub>H<sub>6</sub> (0.54%), C<sub>7</sub>H<sub>8</sub> (0.15%), C<sub>4</sub>H<sub>4</sub> (0.103%), and C<sub>10</sub>H<sub>8</sub> (0.11%), but which were not detected during the experimental tests. In the case of the main compounds such as CO, CO<sub>2</sub>, and CH<sub>4</sub>, proper correlations were found. Some differences between the experimental and numerical results come from some simplifications in the calculation model, for example, constant fuel flow and the residence time in the highest temperature zone. The modelling results showed linear correlation between the temperature and gas component concentrations, without inflexions; the exception was observed for H<sub>2</sub>. In this case, the most plausible reason for the weak correlation between the calculation and experimental results is the experimental procedure. The experimental pyrolytic gas composition collected during the whole experiment was compared to the numerical calculations, and good correlation was achieved for CO and CO<sub>2</sub>. Hydrogen was detected only in the pyrolytic gas after reaching the process temperature. For example, at 600 °C, 10.42% of H<sub>2</sub> was measured in the pyrolytic gas in the second container (see Fig. 9).

The differences in the concentration also come from the assumption of ideal reagent mixing conditions, the initial conditions set in the modelling procedure, and, in particular, the residence time of the reagents in the highest temperature zone. In the experiment, a two-stage process was analysed, and the total sample residence time was the sum of the first and second stages. In the calculations, the residence time

of the sample was set as the time needed to heat the sample to the given process temperature. For 400 °C, the residence time was 1500 s; for 500 °C, 1300 s; and for 600 °C, 1400 s. In the calculations, in contrast to the experiment, a constant mass stream of the analysed biomass was adopted, depending only on the process temperature. Based on the experimental data, the weight loss of the sample was calculated from the time the device reached the set temperature; at 400 °C, the weight loss was  $2,434 \times 10^{-6}$  g/s; at 500 °C,  $3,145 \times 10^{-6}$  g/s, and at 600 °C,  $2,725 \times 10^{-6}$  g/s. All these assumptions and simplifications had an impact on the final correlation between the numerical modelling and experimental results.

The differences between the pyrolytic gas modelling and experimental results also lie in the experimental procedure itself arising from non-ideal mixing, collection of tars prior to gas analysis, not fully closed mass balance, gas collection procedure, possibilities of leakage, and measuring errors of the equipment. The analysis of the formation pathways in the analysed temperature range was performed. A sensitivity analysis in the Ansys Chemkin-Pro software, using the 0-D perfect mixing reactor was conducted. The examined compounds were: H<sub>2</sub>, CO, CO<sub>2</sub>, CH<sub>4</sub>, C<sub>3</sub>H<sub>8</sub>, C<sub>2</sub>H<sub>6</sub>, C<sub>2</sub>H<sub>4</sub>. The analysed variable was the temperature in the range of 400–600 °C. The results of the global sensitive analysis are presented in Table A1 in Supplementary material.

## 4. Conclusions

Biomass waste is a promising energy resource with high potential in Poland. The chemical mechanism of gaseous product formation under the pyrolysis process conditions was explored in detail and the experimental and numerical modelling results were compared. The experimental procedure was performed at process temperatures of 300, 400, 500, and 600 °C. Based on the obtained experimental results, it can be concluded that a higher process temperature leads to an increase in the gas and liquid yields. At 600 °C, the collected tar and gas content was 56.9% and 19.0%, respectively. In the case of char production, the trend was reversed; at 300 °C, 48.0% char was produced, whereas at 600 °C, the value was 24.0%. The solid products had a higher carbon content and the relative H/C and O/C mole ratios changed in comparison to those of the raw materials. The reduction in the O/C ratio enhances the properties of the chars, making the chars a valuable product with high potential in direct fuel combustion or as a raw material for further processing, for example, in activated carbon production. Thermal analysis indicated that the ignition point increased for the chars obtained at higher temperatures; this phenomenon is related to the higher carbon content. Tar analysis showed the presence of two main tar components: acetic acid and isobutyric acid. The liquid phase was also rich in phenolic and aromatic compounds. Analysis of the chars using infrared spectroscopy (FTIR) showed decomposition of the organic matrix with increasing temperature. The quality of the pyrolysis gas increased with temperature, and the highest concentrations of the most valuable compounds such as methane and hydrogen were detected in the pyrolysis gas collected after reactor heat-up at 600 °C. The major components of the pyrolysis gas were CO and CO<sub>2</sub>, but at 600 °C, the concentration of carbon oxide and dioxide started to decrease.

The Ansys Chemkin-Pro software proposed in this article enabled simulation of the oat straw pyrolysis process for given conditions and provided detailed data on the gaseous products. Good correlation between the results of the computer simulations and experimental studies was observed in terms of the main pyrolytic gas components: CH<sub>4</sub>, CO, and CO<sub>2</sub>. In the case of hydrogen and higher hydrocarbons present in the pyrolysis gas in trace amounts, the correlation was weak and the differences between the experimental and modelling results were noticeable. The calculation tool proposed in this study may be helpful for estimating the quality of pyrolysis gas, especially in terms of the major components, for planned and existing installations for thermal waste conversion.

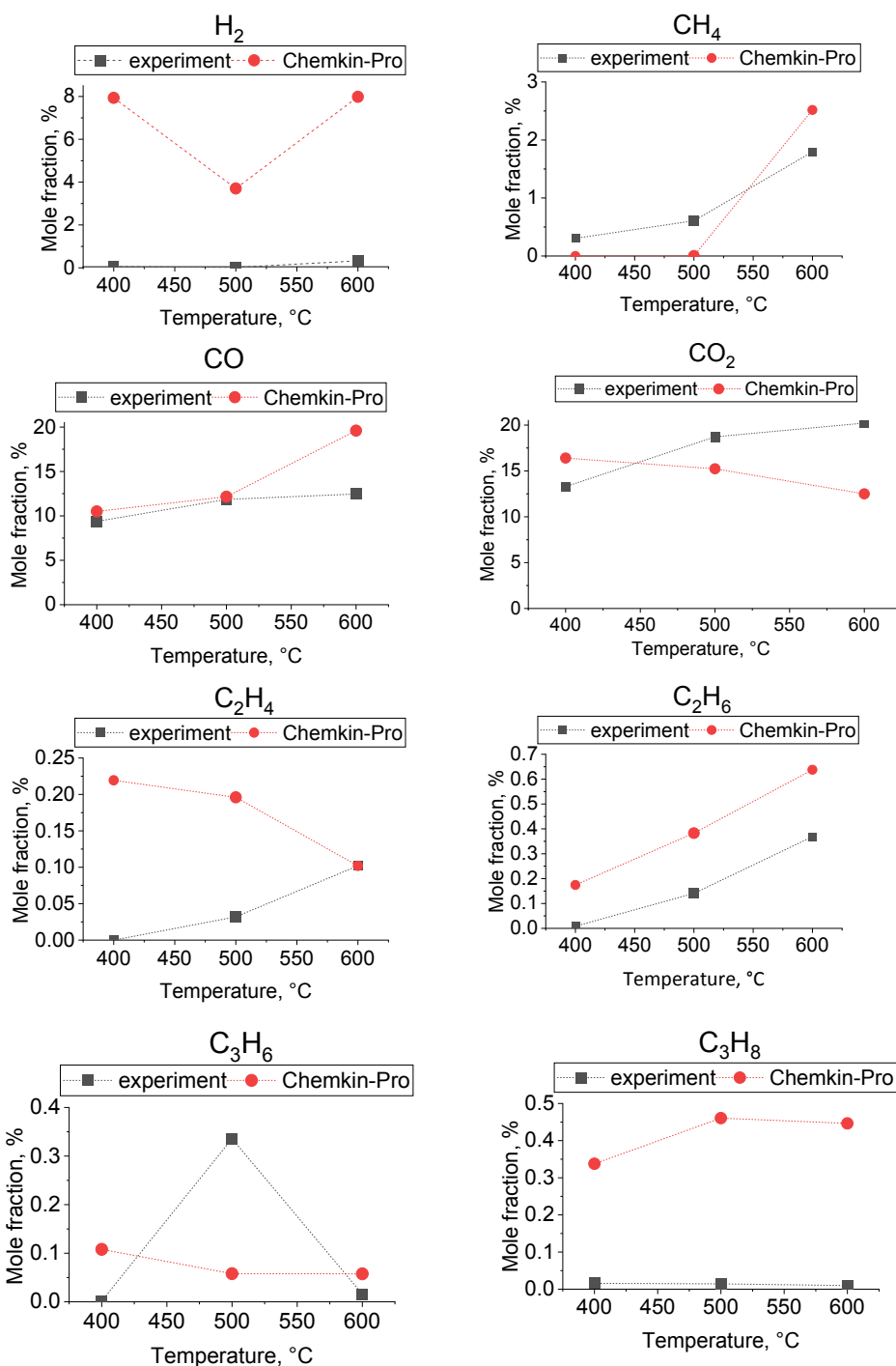


Fig. 10. Comparison of mole fraction of main gaseous products obtained from experiment and modelling results.

#### CRediT authorship contribution statement

**Agata Mlonka-Mędrala:** Conceptualization, Methodology, Formal analysis, Investigation, Writing - original draft, Writing - review & editing. **Panagiotis Evangelopoulos:** Conceptualization, Methodology, Formal analysis, Investigation, Writing - review & editing. **Małgorzata Sieradzka:** Data curation, Investigation, Validation, Writing - review & editing. **Monika Zajemska:** Data curation, Investigation, Validation, Writing - review & editing. **Aneta Magdziarz:** Data curation, Investigation, Validation, Resources, Supervision, Project administration, Writing - review & editing.

#### Declaration of Competing Interest

The authors declare that they have no known competing financial interests or personal relationships that could have appeared to influence the work reported in this paper.

#### Acknowledgements

This project was partially funded by the European Union's Horizon 2020 Research and Innovation Programme under the Marie Skłodowska-Curie grant agreement No. 823745 and the Ministry of Science and Higher Education, Poland [grant AGH no 16.16.110.663].



Additionally, Agata Mlonka-Mędrala would like to kindly thank Weihong Yang from the Department of Materials Science and Engineering, KTH Royal Institute of Technology and BRISK Biofuels Research Infrastructure for Sharing Knowledge.

## Appendix A. Supplementary data

Supplementary data to this article can be found online at <https://doi.org/10.1016/j.fuel.2021.120611>.

## References

- [1] Zeng T, Pollex A, Weller N, Lenz V, Nelles M. Blended biomass pellets as fuel for small scale combustion appliances: effect of blending on slag formation in the bottom ash and pre-evaluation options. *Fuel* 2018;212:108–16. <https://doi.org/10.1016/j.fuel.2017.10.036>.
- [2] Zydin A, Natarajan K, Latva-Käärä P, Iglńska B, Iglńska A, Trishkin M, et al. Estimation of surplus biomass potential in southern and central Poland using GIS applications. *Renew Sustain Energy Rev* 2018;89:204–15. <https://doi.org/10.1016/j.rser.2018.03.022>.
- [3] Kan T, Strezov V, Evans TJ. Lignocellulosic biomass pyrolysis: A review of product properties and effects of pyrolysis parameters. *Renew Sustain Energy Rev* 2016;57:1126–40. <https://doi.org/10.1016/j.rser.2015.12.185>.
- [4] Basu P. Biomass gasification. Pyrolysis and Torrefaction 2018. <https://doi.org/10.1016/c2016-0-04056-1>.
- [5] Mayà JJ, García-Ceballos F, Azuara M, Latorre N, Royo C. Pyrolysis and char reactivity of a poor-quality refuse-derived fuel (RDF) from municipal solid waste. *Fuel Process Technol* 2015;140:276–84. <https://doi.org/10.1016/j.fuproc.2015.09.014>.
- [6] Magdziarz A, Wilk M, Wądrzyk M. Pyrolysis of hydrochar derived from biomass – Experimental investigation. *Fuel* 2020;267:117246. <https://doi.org/10.1016/j.fuel.2020.117246>.
- [7] Das O, Sarmah AK. Value added liquid products from waste biomass pyrolysis using pretreatments. *Sci Total Environ* 2015;538:145–51. <https://doi.org/10.1016/j.scitotenv.2015.08.025>.
- [8] Biswas B, Pandey N, Bisht Y, Singh R, Kumar J, Bhaskar T. Pyrolysis of agricultural biomass residues: comparative study of corn cob, wheat straw, rice straw and rice husk. *Bioresour Technol* 2017;237:57–63. <https://doi.org/10.1016/j.biortech.2017.02.046>.
- [9] Mishra RK, Mohanty K. Kinetic analysis and pyrolysis behaviour of waste biomass towards its bioenergy potential. *Bioresour Technol* 2020;311:123480. <https://doi.org/10.1016/j.biortech.2020.123480>.
- [10] Aqsha A, Tijani MM, Moghtaderi B, Mahinpey N. Catalytic pyrolysis of straw biomasses (wheat, flax, oat and barley) and the comparison of their product yields. *J Anal Appl Pyrolysis* 2017;125:201–8. <https://doi.org/10.1016/j.jaap.2017.03.022>.
- [11] Jaffar MM, Nahil MA, Williams PT. Pyrolysis-catalytic hydrogenation of cellulose-hemicellulose-lignin and biomass agricultural wastes for synthetic natural gas production. *J Anal Appl Pyrolysis* 2020;145:104753. <https://doi.org/10.1016/j.jaap.2019.104753>.
- [12] Ismail TM, Banks SW, Yang Y, Yang H, Chen Y, Bridgwater AV, et al. Coal and biomass co-pyrolysis in a fluidized-bed reactor: numerical assessment of fuel type and blending conditions. *Fuel* 2020;275:118004. <https://doi.org/10.1016/j.fuel.2020.118004>.
- [13] Sieradzka M, Rajca P, Zajemska M, Mlonka-Mędrala A, Magdziarz A. Prediction of gaseous products from refuse derived fuel pyrolysis using chemical modelling software – Ansys Chemkin-Pro. *J Clean Prod* 2020;248:119277. <https://doi.org/10.1016/j.jclepro.2019.119277>.
- [14] Shen W, Zhang Y, Zhao B, Chang D, Lyu J, Zhang H. Experimental and modelling studies on pyrolysis and its main light gas products for typical C8 hydrocarbons. *J Anal Appl Pyrolysis* 2019;142:104622. <https://doi.org/10.1016/j.jaap.2019.05.011>.
- [15] The CRECK Modeling Group. Detailed kinetic mechanisms and CFD of reacting flows n.d. <http://creckmodeling.chem.polimi.it/> (accessed July 6, 2020).
- [16] Lee YR, Choi HS, Park HC, Lee JE. A numerical study on biomass fast pyrolysis process: a comparison between full lumped modeling and hybrid modeling combined with CFD. *Comput Chem Eng* 2015;82:202–15. <https://doi.org/10.1016/j.compchemeng.2015.07.007>.
- [17] Pelucchi M, Cavallotti C, Cuoci A, Faravelli T, Frassoldati A, Ranzi E. Detailed kinetics of substituted phenolic species in pyrolysis bio-oils. *React Chem Eng* 2019;4(3):490–506. <https://doi.org/10.1039/C8RE00198G>.
- [18] Debiagi PEA, Trinchera M, Frassoldati A, Faravelli T, Vinu R, Ranzi E. Algae characterization and multistep pyrolysis mechanism. *J Anal Appl Pyrolysis* 2017;128:423–36. <https://doi.org/10.1016/j.jaap.2017.08.007>.
- [19] Ranzi E, Debiagi PEA, Frassoldati A. Mathematical modeling of fast biomass pyrolysis and bio-oil formation. Note I: Kinetic mechanism of biomass pyrolysis. *ACS Sustain Chem Eng* 2017;5(4):2867–81. <https://doi.org/10.1021/acssuschemeng.6b03096>.
- [20] Dhahak A, Bounaceur R, Le Dreff-Lorimier C, Schmidt G, Trouve G, Battin-Leclerc F. Development of a detailed kinetic model for the combustion of biomass. *Fuel* 2019;242:756–74. <https://doi.org/10.1016/j.fuel.2019.01.093>.
- [21] Qi G, Wang Z, Zhang S, Dong Y, Guan J, Dong P. Numerical simulation on biomass-pyrolysis and thermal cracking of condensable volatile component. *Int J Hydrogen Energy* 2020;45(22):12283–97. <https://doi.org/10.1016/j.ijhydene.2020.02.199>.
- [22] Wang X, Hu M, Hu W, Chen Z, Liu S, Hu Z, et al. Thermogravimetric kinetic study of agricultural residue biomass pyrolysis based on combined kinetics. *Bioresour Technol* 2016;219:510–20. <https://doi.org/10.1016/j.biortech.2016.07.136>.
- [23] Hu M, Wang X, Chen J, Yang P, Liu C, Xiao Bo, et al. Kinetic study and syngas production from pyrolysis of forestry waste. *Energy Convers Manag* 2017;135:453–62. <https://doi.org/10.1016/j.enconman.2016.12.086>.
- [24] Mlonka-Mędrala A, Golombek K, Buk P, Cieślak E, Nowak W. The influence of KCl on biomass ash melting behaviour and high-temperature corrosion of low-alloy steel. *Energy* 2019;188:116062. <https://doi.org/10.1016/j.energy.2019.116062>.
- [25] Gadek W, Mlonka-Mędrala M, Prestipino M, Evangelopoulos P, Kalisz S, Yang W, et al. Gasification and pyrolysis of different biomasses in lab scale system: a comparative study. *E3S Web Conf* 2016;10:00024. <https://doi.org/10.1051/e3sconf/20161000024>.
- [26] Zajemska M, Rajca P, Szwaja S, Morel S. The chemical mechanism of the HCL formation in the pyrolysis process of selected wastes. *Przem Chem* 2019;98:907–10. <https://doi.org/10.15199/62.2019.6.8>.
- [27] Che D, Li S, Yang W, Jia J, Zheng N. Application of numerical simulation on biomass gasification. *Energy Procedia* 2012;17:49–54. <https://doi.org/10.1016/j.egypro.2012.02.061>.
- [28] Ye Z, Liu L, Tan Z, Zhang L, Huang Q. Effects of pyrolysis conditions on migration and distribution of biochar nitrogen in the soil-plant-atmosphere system. *Sci Total Environ* 2020;723:138006. <https://doi.org/10.1016/j.scitotenv.2020.138006>.
- [29] Hwang I-H, Kobayashi J, Kawamoto K. Characterization of products obtained from pyrolysis and steam gasification of wood waste, RDF, and RPF. *Waste Manag* 2014;34(2):402–10. <https://doi.org/10.1016/j.wasman.2013.10.009>.
- [30] Botelho T, Costa M, Wilk M, Magdziarz A. Evaluation of the combustion characteristics of raw and torrefied grape pomace in a thermogravimetric analyzer and in a drop tube furnace. *Fuel* 2018;212:95–100. <https://doi.org/10.1016/j.fuel.2017.09.118>.
- [31] Mihajlović M, Petrović J, Maletić S, Isakovski MK, Stojanović M, Lopičić Z, et al. Hydrothermal carbonization of Miscanthus × giganteus: Structural and fuel properties of hydrochars and organic profile with the ecotoxicological assessment of the liquid phase. *Energy Convers Manag* 2018;159:254–63. <https://doi.org/10.1016/j.enconman.2018.01.003>.
- [32] Peng C, Zhai Y, Zhu Y, Xu B, Wang T, Li C, et al. Production of char from sewage sludge employing hydrothermal carbonization: Char properties, combustion behavior and thermal characteristics. *Fuel* 2016;176:110–8. <https://doi.org/10.1016/j.fuel.2016.02.068>.
- [33] Muvhiwa R, Kuvarega A, Llana EM, Muleja A. Study of biochar from pyrolysis and gasification of wood pellets in a nitrogen plasma reactor for design of biomass processes. *J Environ Chem Eng* 2019;7(5):103391. <https://doi.org/10.1016/j.jece.2019.103391>.
- [34] Mathanker A, Pudasainee D, Kumar A, Gupta R. Hydrothermal liquefaction of lignocellulosic biomass feedstock to produce biofuels: Parametric study and products characterization. *Fuel* 2020;271:117534. <https://doi.org/10.1016/j.fuel.2020.117534>.
- [35] He C, Giannis A, Wang JY. Conversion of sewage sludge to clean solid fuel using hydrothermal carbonization: Hydrochar fuel characteristics and combustion behavior. *Appl Energy* 2013;111:257–66. <https://doi.org/10.1016/j.apenergy.2013.04.084>.
- [36] Müsellim E, Tahir MH, Ahmad MS, Ceylan S. Thermokinetic and TG/DSC-FTIR study of pea waste biomass pyrolysis. *Appl Therm Eng* 2018;137:54–61. <https://doi.org/10.1016/j.applthermaleng.2018.03.050>.
- [37] Li J, Tian Y, Zong P, Qiao Y, Qin S. Thermal cracking behavior, products distribution and char/steam gasification kinetics of seawater Spirulina by TG-FTIR and Py-GC/MS. *Renew Energy* 2020;145:1761–71. <https://doi.org/10.1016/j.renene.2019.07.096>.
- [38] Bahng M-K, Mukarakate C, Robichaud DJ, Nimlos MR. Current technologies for analysis of biomass thermochemical processing: a review. *Anal Chim Acta* 2009;651(2):117–38. <https://doi.org/10.1016/j.aca.2009.08.016>.
- [39] Evangelopoulos P, Sophonrat N, Jilvero H, Yang W. Investigation on the low-temperature pyrolysis of automotive shredder residue (ASR) for energy recovery and metal recycling. *Waste Manag* 2018;76:507–15. <https://doi.org/10.1016/j.wasman.2018.03.048>.
- [40] Moldoveanu SC. Chapter 19 Pyrolysis of Various Derivatives of Carboxylic Acids. vol. 28. 2010. [https://doi.org/10.1016/S0167-9244\(09\)02819-4](https://doi.org/10.1016/S0167-9244(09)02819-4).
- [41] Demirbas A. The influence of temperature on the yields of compounds existing in bio-oils obtained from biomass samples via pyrolysis. *Fuel Process Technol* 2007;88(6):591–7. <https://doi.org/10.1016/j.fuproc.2007.01.010>.
- [42] Moldoveanu SC. Chapter 9 Pyrolysis of alcohols and phenols. *Tech Instrum Anal Chem*, vol. 28, 2010, p. 259–313. doi: 10.1016/S0167-9244(09)02809-1.
- [43] Yerrayya A, Natarajan U, Vinu R. Fast pyrolysis of guaiacol to simple phenols: Experiments, theory and kinetic model. *Chem Eng Sci* 2019;207:619–30. <https://doi.org/10.1016/j.ces.2019.06.025>.

- [44] Awasthi A, Singh G, Dhyani V, Kumar J, Reddy YS, Adarsh VP, et al. Co-pyrolysis of phumdi and para grass biomass from Loktak Lake. *Bioresour Technol* 2019;285: 121308. <https://doi.org/10.1016/j.biortech.2019.03.147>.
- [45] Ren S, Lei H, Wang Lu, Bu Q, Chen S, Wu J, et al. The effects of torrefaction on compositions of bio-oil and syngas from biomass pyrolysis by microwave heating. *Bioresour Technol* 2013;135:659–64. <https://doi.org/10.1016/j.biortech.2012.06.091>.
- [46] Shen Y, Li X, Yao Z, Cui X, Wang CH. CO<sub>2</sub> gasification of woody biomass: experimental study from a lab-scale reactor to a small-scale autothermal gasifier. *Energy* 2019;170:497–506. <https://doi.org/10.1016/j.energy.2018.12.176>.